III. Results

Computer programs were written which implement (1) and (2) separately for the magnetic and electric wall cases. The programs compute the determinant of the matrix as a function of the unknown transverse wavenumber. The eigenvalue is determined by noting a change of sign between successive determinant values and then using quadratic interpolation. This scheme is simple to implement, and very accurate results can be obtained when the frequency axis is sampled sufficiently densely. Although this dense sampling requirement means that the method is computationally intensive, it also means that eigenvalues which are nearly degenerate are more likely to be found.

Figs. 3 and 4 illustrate the results we obtain when we apply our analysis to the geometry illustrated in the insets to the figures. (This geometry is the only case which was analyzed by both previous groups and therefore provides a meaningful case for comparisons between them.) Fig. 3 is a direct comparison between our results and those of Zhang and Joines, plotted on the scale used in [7]. The disagreement is quite large and is increasing as the value of the parameter (s/a) increases. Fig. 4 is a direct comparison between our results and those of Mazumder and Saha, plotted on the scale used in [6]. Although small discrepancies remain, it is clear that our results are in agreement with [6] and with the new results reported in [10].

In order to understand the source of the discrepancy between the references we tried plotting several other cases. Fig. 5 is our most successful attempt. The solid lines again indicate the bandwidth as reported in [7] and the symbols indicate the bandwidth defined by the difference in eigenvalues of the first two solutions associated with a magnetic wall in what we call region 1. These two modes are the first and third propagating modes of the structure.

Fig. 6 illustrates the transverse electric field lines for several values of (s/a) for the first two electric wall modes for one particular case $(t/b = 0.10)$ for the geometry investigated above. It is clear that in the limit as $s/a \rightarrow 0.0$ the waveguide becomes rectangular and these two modes reduce to the standard TE_{01} and TE_{20} modes. (In this limit the width of the base of the "T" must also go to zero.) As the parameter (s/a) increases, perturbation theory tells us that the modes become mixed and these simple labels are no longer meaningful. Although some resemblance to the TE_{20} field distribution appears in both cases, it is clear that using such labels is incorrect and may be misleading. It is, of course, equally incorrect to label the dominant mode as the TE_{10} and we have refrained from so doing. We prefer simply to label the modes in ascending order of cutoff frequency, i.e. TE_1, $TE_2, \cdots$, etc. However, we recognize that other schemes, such as that proposed in [9], may be more desirable in certain situations.

IV. Conclusions

The single T-septum waveguide has been analyzed using the Rayleigh–Ritz–Galerkin technique. The method is a variation of that used by two previous groups who reported conflicting results. The results of the new analysis agree closely with those of Mazumder and Saha [5], [6] and those of German and Riggs [10] and disagree with those of Zhang and Joines [7], [8]. The history of T-septum waveguide has been discussed.

References

[1] R. S. Elliott, "Two-mode waveguide for equal mode velocities," *IEEE Trans. Microwave Theory Tech.*, vol. MTT-16, pp. 282–286, May 1968.

[2] P. Silvester, "A general high-order finite element waveguide analysis program," *IEEE Trans. Microwave Theory Tech.*, vol. MTT-17, pp. 204–210, Apr. 1969.

[3] N. G. Alexopoulos and N. E. Armstrong, "Two-mode waveguide for equal mode velocities—correction," *IEEE Trans. Microwave Theory Tech.*, vol. MTT-21, pp. 157–158, Mar. 1973.

[4] R. W. Lyon, "An investigation of apertures in dual mode rectangular waveguide for variable polarization arrays," PhD dissertation, Dept. of Electrical and Electronic Engineering, Heriot-Watt University, Scotland, 1979.

[5] G. G. Mazumder and P. K. Saha, "A novel rectangular waveguide with double T-septums," *IEEE Trans. Microwave Theory Tech.*, vol. MTT-33, pp. 1235–1238, Nov. 1985.

[6] G. G. Mazumder and P. K. Saha, "Rectangular waveguide with T-shaped septa," *IEEE Trans. Microwave Theory Tech.*, vol. MTT-35, pp. 201–204, Feb. 1987.

[7] Y. Zhang and W. T. Joines, "Some properties of T-septum waveguides," *IEEE Trans. Microwave Theory Tech.*, vol. MTT-35, pp. 769–775, Aug. 1987.

[8] Y. Zhang and W. T. Joines, "Attenuation and power handling capability of T-septum waveguides," *IEEE Trans. Microwave Theory Tech.*, vol. MTT-35, pp. 858–861, Sept. 1987.

[9] J. P. Montgomery, "On the complete eigenvalue spectrum of ridged waveguide," *IEEE Trans. Microwave Theory Tech.*, vol. MTT-19, pp. 547–555, June 1971.

[10] F. J. German and L. S. Riggs, "Bandwidth properties of rectangular T-Septum waveguides," pp. 917–919, this issue.

[11] D. Dasgupta and P. K. Saha, "Eigenvalue spectrum of waveguide with two symmetrically placed double ridges," *IEEE Trans. Microwave Theory Tech.*, vol. MTT-29, pp. 47–51, Jan. 1981.

[12] D. Dasgupta and P. K. Saha, "Rectangular waveguide with two double ridges," *IEEE Trans. Microwave Theory Tech.*, vol. MTT-31, pp. 938–941, Nov. 1983.

[13] B. E. Paulis, "Analysis of an infinite array of waveguides with a pair of double ridges," presented at the 1987 IEEE AP-S Meeting, Blacksburg, VA, June 15–19, 1987.

[14] S. W. Lee, W. R. Jones, and J. J. Campbell, "Convergence of iris-type discontinuity problems," *IEEE Trans. Microwave Theory Tech.*, vol. MTT-19, pp. 528–536, June 1971.

Optimized Method for Obtaining Permittivity and Conductivity Profiles of Microwave Materials

MOATAZA A. HINDY

***Abstract*—A new iterative method for obtaining the distribution of the relative permittivity $\epsilon_r(z)$ or electrical conductivity $\sigma(z)$ of microwave semiconducting materials is presented. The semiconducting material is fitted in a rectangular waveguide which is terminated by a variable short circuit. The reflection coefficients of the system are measured at a single frequency and at different positions of the moving short. The measured coefficients are used in the iterative process of solving the inverse problem by obtaining the functional gradient [1], [2]. The method takes into account continuous and discontinuous profiles.**

I. Introduction

Previously the solutions of the ill-posed electromagnetic inverse problems were discussed by Morozov [3] and Tikhonov [4]. Electromagnetic probing of an inhomogeneous stratified medium using time- and spectral-domain analyses of reflection coefficients is presented by Bolomey *et al.* [5]. The computed results are in general oscillating. The optimization technique is used with the direct method and the minimum of the cost function is reached after 65 iterations, which is large. The main drawbacks of the time- and spectral-domain methods are with discontinuous profiles. Approximate construction of the dielectric constant pro-

Manuscript received January 23, 1988; revised November 2, 1988.

The author is with the Electronics Research Institute, National Research Centre, Cairo, Egypt.

IEEE Log Number 8826039.

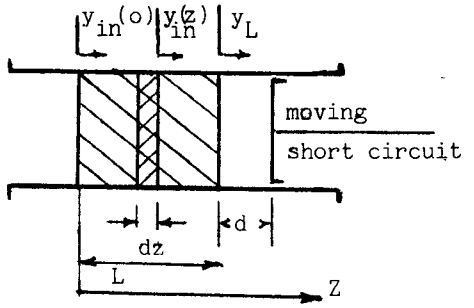

Fig. 1. The inhomogeneous layer is fitted in a waveguide.

file from its impulse response is discussed in [6], while in [7] an iterative scheme in functional space is presented using the reflected power for a set of discrete frequencies.

In this paper the iterative functional gradient method (FGM) [1], [2] is applied to determine the profiles of $\epsilon'(z)$ and $\sigma(z)$ for a semiconducting layer at microwave frequency. A variable load technique is used rather than variations in frequency, due to the fact that microwave generators and waveguides have narrow frequency bands. But informative measurements, needed for solving such an inverse problem, require a wide band of frequency.

II. Analysis of the Functional Gradient Method

Consider the experimental setup of the problem in Fig. 1. The input admittance $y_{in}(z)$ at the incremental layer dz is

$$y_{in}(z) = y(z)\frac{(y_{in}(z)+dy_{in}(z))+y(z)\tanh(\gamma(z)\,dz)}{y(z)+(y_{in}(z)+dy_{in}(z))\tanh(\gamma(z)\,dz)} \quad (1)$$

where $y(z)$ and $\gamma(z)$ are, respectively, the normalized guided wave admittance and the complex propagation constant in the layer dz:

$$y(z) = \left(\mu_k(Z)\epsilon_k(z)-(\lambda_0/\lambda_c)^2\right)^{1/2}/\left(1-(\lambda_0/\lambda_c)^2\right)^{1/2} \quad (1a)$$

$$\gamma(z) = j\omega\left(\mu_k(z)\epsilon_k(z)-(\lambda_0/\lambda_c)^2\right)^{1/2}(\mu_0\epsilon_0)^{1/2} \quad (1b)$$

$$\mu_k(z)=1 \qquad \epsilon_k=\epsilon_r+j\epsilon''.$$

Obtaining the real and imaginary parts of (1a) and (1b), we get

$$y(z) = A_1(C(z)-jD(z))$$

$$\gamma(z) = A_2(D(z)+jC(z))$$

$$c(z) = \left[\left(\epsilon'^2(z)+\epsilon''^2(z)\right)^{1/2}+\epsilon'(z)\right]^{1/2}$$

$$D(z) = \left[\left(\epsilon'^2(z)+\epsilon''^2(z)\right)^{1/2}-\epsilon'(z)\right]^{1/2}$$

$$A_1 = \left[2\left(1-(\lambda_0/\lambda_c)^2\right)\right]^{1/2}$$

$$A_2 = \sqrt{2}\,\pi/\lambda_0$$

$$\epsilon'(z) = \epsilon_r(z)-\left(\frac{\lambda_0}{\lambda_c}\right)^2$$

$$\epsilon''(z) = \sigma(z)/\epsilon_0\omega.$$

Here λ_0 and ϵ_0 are the free-space wavelength and the permittivity, respectively, λ_c is the cutoff wavelength of the waveguide, and ω is the angular frequency. If dz is chosen as small as possible, (1) will have the form

$$\frac{dy_{in}(z)}{dz} = -2A_1A_2\frac{\sigma(z)}{\omega_0}+jA_2\left(\frac{y_{in}^2(z)}{A_1}-2A_1\epsilon'(z)\right). \quad (2)$$

In [8] cases of dielectrics and semiconductors with one inhomogeneous parameter are considered. In this paper cases of materials with two inhomogeneous parameters $(\epsilon_r(z), \sigma(z))$ will be discussed.

III. Case of an Inhomogeneous Semiconductor Having Unknown $\epsilon_r = f(z)$ and Known $\sigma = f(z)$

We suggest an initial solution $\epsilon'(z)$. The corresponding calculated reflection coefficient is Re^{jQ} and the real measured reflection coefficient is $R_re^{jQ_r}$. The functional $\rho[\epsilon'(z)]$, which evaluates the difference between measured and calculated coefficients for N positions of the short circuit (S.C.), has the form

$$\rho[\epsilon'(z)] = \sum_{n=1}^{N}\left|\left(R_{r,n}e^{jQ_{r,n}}-R_ne^{jQ_n}\right)\right|^2 \quad (3)$$

where n is related to the order number of measurement.

If the initial solution is assumed to be of the form

$$\epsilon'_m(z) = \epsilon'(z)+h\epsilon'_{cr}(z) \quad (4)$$

where $\epsilon'_{cr}(z)$ is a corrective function and h is a modifying parameter, the corresponding admittance change is

$$y_m(z) = y_{in}(z)+hy_{cr}(z). \quad (5)$$

Equation (5) must satisfy the Riccati equation, (2); hence from (2), (4), and (5) and neglecting the terms containing h^2 we get

$$-j\frac{dy_{cr}(z)}{dz} = 2B_1y_{in}(z)y_{cr}(z)-B_2\epsilon'_{cr}(z) \quad (6)$$

with the condition $y_{cr}(L)=0$, and

$$B_1 = A_2/A_1 \qquad B_2 = 2A_1A_2.$$

Solution of (6) has the form

$$y_{cr}(z) = jB_2\int_Z^L\epsilon'_{cr}(v)\cdot e^{j\delta-j2B_1y_{in}(u,d)\,du}\,dv. \quad (7)$$

The gradient of the functional (3) is

$$\Delta\rho[\epsilon'(z)] = \sum_{n=1}^{N}2\mathrm{Re}[\Delta S_n(S_{i,n}^*-S_n^*)] \quad (8)$$

where

$$S = Re^{jQ}$$

$$\Delta S = -2\Delta y_{in}(0)/(1+y_{in}(0))^2$$

$$= \frac{-2jB_2}{(1+y_{in}(0))^2}\int_0^L h\epsilon'_{cr}(z)\,e^{-j2B_2\int_0^z y_{in}(u,d)\,du}\,dz. \quad (9)$$

From (8) and (9) we get

$$\Delta\rho[\epsilon'(z)] = \int_0^L G(z)h\epsilon'_{cr}(z)\,dz \quad (10)$$

where

$$G(z) = \sum_{n=1}^{N}\mathrm{Re}\left[\frac{j4B_2(S_{i,n}^*-S_n^*)}{(1+y_{in}(0))^2}e^{-j2B_1\int_0^z y_{in}(u,d)\,du}\right]. \quad (11)$$

From the condition of a minimum functional [1]–[3] we have

$$h\epsilon'_{cr}(z) = -tG(z). \quad (12)$$

The new corrected solution is

$$\epsilon'_m(z) = \epsilon'(z) - tG(z) \tag{13}$$

where t is a modifying optimizing parameter, which must satisfy the condition

$$\min_t \rho\left[Re^{jQ}(\epsilon'(z) - tG(z))\right]. \tag{14}$$

Using a suitable minimizing technique one can choose the optimum value of t which minimizes the functional ρ of (14).

Starting again from $\epsilon'_m(z)$ as an initial solution, the iterative cycle is repeated until we have

$$\rho|\epsilon'_m(z)| \leqslant \pm\delta$$

where δ is within the allowable range of error.

IV. Case of Semiconductor Which Has Known $\epsilon_r(z)$ and Unknown $\sigma(z)$

The corresponding differential equation which determines the corrective function $\sigma_{cr}(z)$ is

$$\frac{dy_{cr}(z)}{dz} = j2B_1 y_{in}(z)\, y_{cr}(z) - \frac{B_2}{\omega\epsilon_0}\sigma_{cr}(z). \tag{15}$$

Solving (15) we get

$$y_{cr}(0) = \frac{B_2}{\omega\epsilon_0}\int_0^L \sigma_{cr}(z)\, e^{-j2B_1\int_0^z y_{in}(u,d)\,du}\, dz. \tag{16}$$

Following the same steps as with (8)–(10) we obtain an expression for the functional gradient:

$$\Delta\rho[\sigma(z)] = \int_0^L D(z)\, h\sigma_{cr}(z)\, dz \tag{17}$$

where

$$D(z) = \sum_{n=1}^{N} \frac{4B_2}{\omega\epsilon_0}\,\mathrm{Re}\left[\frac{(S^*_{r,n} - S^*_n)}{(1+y_{in,n}(0))^2}\, e^{-j2B1\int_0^z y_{in,n}(u,d)\,du}\right] \tag{18}$$

and from the condition of the minimum functional,

$$h\sigma_{cr}(z) = -tD(z) \tag{19}$$

and the new corrected solution,

$$\sigma_m(z) = \sigma(z) - tD(z) \tag{20}$$

t is selected by an optimizing program to satisfy the condition

$$\min_t \rho[S(\sigma(z) - tD(z))]. \tag{21}$$

V. Numerical Examples

Example 1

A semiconducting material has known $\epsilon'(z)$ and unknown $\sigma(z)$ of the forms

$$\epsilon'(z) = Z/L + 4$$

$$\sigma(z) = 9\exp(-1.5Z/L)\ (\Omega\cdot\mathrm{m})^{-1}.$$

Two suggested initial solutions are tried (Fig. 2):

$$\sigma_1(z) = 4 - 2.5Z/L\ (\Omega\cdot\mathrm{m})^{-1}$$

$$\sigma_2(z) = 9 - 7Z/L\ (\Omega\cdot\mathrm{m})^{-1}$$

where $Z/L \in [0;1]$, $N = 17$. Using $\sigma_1(z)$ and $\sigma_2(z)$ the final solutions $S_1(z)$ and $S_2(z)$ are obtained after seven and three cycles of iterations, respectively, at a single frequency of 32 GHz. For the real profile $\sigma_a(z)$ with a discontinuity at $Z/L = 0.5$,

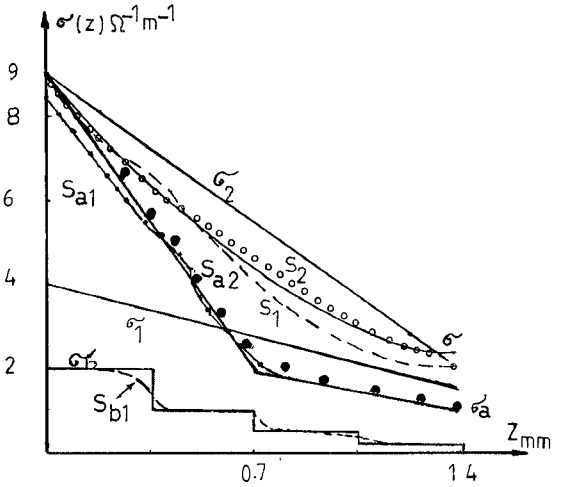

Fig. 2 σ, σ_a, and σ_b are real distributions. σ_1 and σ_2 are initial profiles. S_1, S_2, S_{a1}, S_{a2}, and S_{b1} are the solutions obtained.

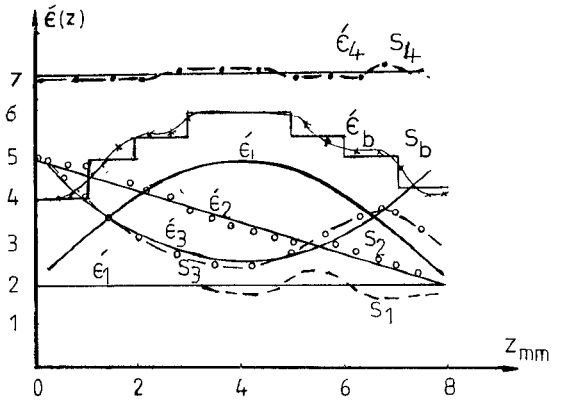

Fig. 3. ϵ'_1, ϵ'_2, ϵ'_3 ϵ'_4, and ϵ'_b are real profiles. ϵ'_i is the initial solution. S_1, S_2, S_3, S_4, and S_b are the solutions obtained.

profiles $Sa_1(z)$ and $Sa_2(z)$ are obtained after 11 and five iterations, respectively. For the real pulsating distribution $\sigma_b(z)$, the solution $S_{b1}(z)$ is reached after three cycles.

Example 2

Fig. 3 illustrates the solution for four cases of materials which have the same known conductivity, $\sigma(z) = Z/L + 1\ (\Omega\cdot\mathrm{m})^{-1}$ and different unknown permittivity:

$$\epsilon'_1(z) = 2 \qquad \epsilon'_2(z) = 5 - 3Z/L$$

$$\epsilon'_3(z) = 2.5 + 10(Z/L - 0.5)^2 \qquad \epsilon'_4(z) = 7.$$

The four samples have the same thickness (0.8 cm). Each is fitted in a waveguide and the reflection coefficients (due to 16 load variations) are measured at a single frequency of 9.4 GHz. For each of the four problems, only one initial solution $\epsilon'_i(z)$ is suggested:

$$\epsilon'_i(z) = 5\exp\left[-0.8(2z/L - 1)^2\right].$$

The solutions $S_1(z)$, $S_2(z)$, $S_3(z)$, and $S_4(z)$ are obtained for $\epsilon'_1(z)$, $\epsilon'_2(z)$, $\epsilon'_3(z)$, and $\epsilon'_4(z)$ after six, five, 11, and seven iterative cycles, respectively. The reconstruction accuracy decreases for points close to the farthest interface because the initial solution differs greatly from the real, and additional regularization cycles are needed with a modified functional. This is done in reconstructing $\epsilon'_2(z)$ and $\epsilon'_4(z)$ (Fig. 3) and better accuracy is

TABLE I

Z mm	0	0.002	0.004	0.005	0.01	0.02	0.03	0.04	0.05	0.1	0.5	1	1.5	2	3
Real $\sigma(z)$ $(ohm.m)^{-1}$	33	26	16	10	6	2.3	1.25	0.75	0.5	0.2	0.2	0.2	0.2	0.2	0.2
Initial $\sigma(z)$ $(ohm.m)^{-1}$	35	32	30	27	22	13	8	4.75	4	0.4	0.4	0.4	0.4	0.4	0.4
Reached $\sigma_1(z)$ $(ohm.m)^{-1}$	33.2	26.2	16.5	11	6.5	2.5	1.25	0.75	0.5	0.25	0.22	0.21	0.22	0.22	0.22

realized after one cycle. For the real pulsating $\epsilon_b'(z)$ a solution $S_b(z)$ is reached after four iterations.

Example 3

Table I illustrates the application of the gradient technique for obtaining the conductivity profile of a lossy semiconductor which has $\epsilon'(z) = 12 - Z/L$ and unknown inhomogeneous $\sigma(z)$. The layer thickness is 3 mm, $N = 16$, and the frequency is 10 GHz. From the table it is clear that the obtained $\sigma_1(z)$ distribution is very close to the real one. The only limitation, on solving for semiconductors having high parameter values, is to optimize the layer thickness by

$$\bar{\lambda}/4 < L < \bar{\lambda}/2$$

where $\bar{\lambda}$ is the average wavelength in the tested sample. This limitation ensures that variations in the measured reflection coefficients are due to load variations.

VI. Discussion and Conclusions

It is clear from the above numerical experiments that the iterative technique of the FGM is very efficient in determining the inhomogeneous profile of the complex dielectric constant of materials. The functional reaches its global minimum in a finite number of iterative cycles and the final solution obtained is unique and independent of the initial guess. One need not have *a priori* information about the medium, but only information about the maximum and minimum values of the desired function. The FGM does not have restrictions on the initial solution and it is applicable with good approximations to discontinuous functions. The number of measurements N must be sufficient to give true information about the probed medium, and optimum N is given by $20 > N > 12$. All the N measurements are carried out at a single frequency. The frequency error (Δf) must not exceed 5 percent. At 36.524 GHz (for a medium which has an average $\epsilon'(z) = 12$ and $\sigma(z) = 5$), $\Delta f = \pm 6$ percent will cause errors in the evaluated reflection coefficients; $\Delta R = \pm 3.5$ percent and $\Delta Q = \pm 8.477$ percent. The corresponding errors in the reconstructed $\epsilon'(z)$ and $\sigma(z)$ are ± 4.55 percent and ± 8.3 percent, respectively. These error values will differ for different materials.

References

[1] A. V. Tikhonravov, "Synthesis problem of stratified medium having a function distribution of parameters," *Sov. Opt. Spectroscopy*, vol 24, no. 6, pp. 1185–190, 1977.

[2] T. K Sarkar, E. Arvas, and S. M Reo, "Application of FFT and the conjugate gradient method for the solution of electromagnetic radiation from electrically large and small conducting bodies," *IEEE Trans. Antennas Propagat*, vol. AP-34, pp. 635–640, May 1986

[3] V. A. Morozov, *Methods for Solving Incorrectly Posed Problems*. New York: Springer-Verlag, 1984.

[4] A. N. Tikhonov and V. U. Arcenin, *Methods of Solving Incorrect Problems* Moscow: Nauka, 1979.

[5] J. C. Bolomey, D. Lesselier, C. Pichot, and W. Tabbara, "Spectral and time domain approaches to some inverse scattering problems," *IEEE Trans. Antennas Propagat.*, vol. AP-29, pp. 206–212, Mar. 1981

[6] S. Coen, "Inverse scattering of a layered and dispersionless dielectric half-space, Part 1: Reflection data from plane wave at normal incidence," *IEEE Trans Antennas Propagat*, vol. AP-29, pp. 726–732, Sept 1981.

[7] A. G. Tijhuis and C Van Der Worm, "Iterative approach to the frequency-domain solution of the inverse-scattering problem for an inhomogeneous lossless dielectric slab," *IEEE Trans. Antennas Propagat.*, vol AP-32, pp. 711–716, July 1984.

[8] M A. Hindy, "Gradient method for the solution of microwave inverse problems of semiconductors," presented at 29th Midwest Symp. Circuits Syst., 1986.

Transmission Properties of a Right-Angle Microstrip Bend with and Without a Miter

ANTONIOS D. BROUMAS, HAO LING, MEMBER, IEEE, AND TATSUO ITOH, FELLOW, IEEE

Abstract **— Based on the waveguide model, the transmission properties of a microstrip bend with and without a miter are investigated using the Green's theorem approach. Unlike the conventional mode-matching technique, this approach does not require a modal description of fields inside the discontinuity region. Scattering parameters for the bend are presented. They agree well with the quasi-static results at low frequencies. Significant improvement in the transmission properties is observed for the bend with a miter.**

I. Introduction

A right-angle microstrip bend is one of the most common discontinuities encountered in microstrip-based integrated circuits. It is normally used to provide flexibility in circuit layout. Accurate characterization of the transmission properties of a microstrip bend therefore plays an important role in the success-

Manuscript received June 6, 1988; revised November 21, 1988 This work was supported by the National Science Foundation under Grant ECS-8657524 and by the Army Research Office under Contract DAAL 03-88-K-0005.

The authors are with the Department of Electrical and Computer Engineering, University of Texas at Austin, Austin, TX 78712

IEEE Log Number 8926578.